

High order discontinuous Galerkin methods for hyperbolic conservation laws with source terms: Part II

Yulong Xing

Department of Mathematics
Ohio State University
xing.205@osu.edu
<https://people.math.osu.edu/xing.205/>

Lectures Series on High-Order Numerical Methods, Aug 7, 2020



THE OHIO STATE
UNIVERSITY

Outline

- 1 Euler equations with gravitational field
- 2 Blood Flow
- 3 Shallow water equations with horizontal temperature gradients (Ripa models)
- 4 Other examples of hyperbolic balance laws
- 5 Summary

Hyperbolic balance laws

- Hyperbolic balance laws (hyperbolic systems of conservation laws with source terms arising from geometrical, reactive, biological or other considerations):

$$U_t + f(U)_x = s(U, x)$$

- **Applications** in different fields including chemistry, biology, fluid dynamics, astrophysics, and meteorology.
- **Examples:** pollutant transport, sediment transport, chemical reaction, chemosensitive movement, shallow water flows, gas dynamics with gravity, nearly hydrostatic flow in climate modeling, etc.

Hyperbolic balance laws

- Hyperbolic balance laws

$$U_t + f(U)_x = s(U, x)$$

Steady state solution, i.e. solution of $f(U)_x = s(U, x)$.

- Standard numerical schemes usually fail to capture the steady state well and introduce **spurious oscillations**. The grid must be **extremely refined** to reduce the size of these oscillations.
- **Well-balanced methods** are developed to reduce the unnecessarily refined mesh. They are specially designed to preserve exactly these steady-state solutions up to machine error with relatively coarse meshes.

A typical example of balance laws

Shallow water equations (SWEs) with a non-flat bottom topography:

$$h_t + (hu)_x = 0$$

$$(hu)_t + \left(hu^2 + \frac{1}{2}gh^2 \right)_x = -ghb_x$$

- h : water height; u : velocity;
 b : bottom topography; g : gravitational constant.

- Still water at rest steady state:

$$u = 0 \quad \text{and} \quad h + b = \text{const.}$$

Moving water steady state:

$$hu = \text{const} \quad \text{and} \quad u^2/2 + g(h + b) = \text{const.}$$

- Extensive well-balanced methods have been developed in the past two decades.

Numerical challenge

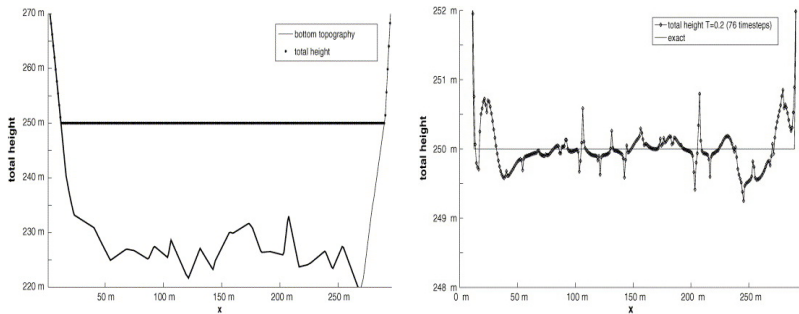


Figure: Numerical computation of Lake Rursee with 296 cells. Left: bottom topography and still water level at time $T = 0$; Right: water level at time $T = 0.2$ (76 time steps) by standard methods. **Note the spurious oscillations** on the right figure. (Credit: S. Noelle et al.)

Euler equations with a gravitational potential

Euler equations with a source term due to the static gravitational field:

$$\begin{aligned}\rho_t + \nabla \cdot (\rho \mathbf{u}) &= 0, \\ (\rho \mathbf{u})_t + \nabla \cdot (\rho \mathbf{u} \otimes \mathbf{u} + p \mathbf{I}_d) &= -\rho \nabla \phi, \\ E_t + \nabla \cdot ((E + p) \mathbf{u}) &= -\rho \mathbf{u} \cdot \nabla \phi,\end{aligned}$$

- ρ : fluid density; \mathbf{u} : velocity; p : pressure;
 $E = \frac{1}{2} \rho u^2 + p/(\gamma - 1)$: non-gravitational energy.
- $\phi = \phi(\mathbf{x})$: time independent gravitational potential.
A simple example is: $\phi_z = g$.
- The hydrostatic balance with a zero velocity:

$$\rho = \rho(x), \quad u = 0, \quad \nabla p = -\rho \nabla \phi,$$

where the flux produced by the pressure balances the gravitational source.

Small perturbation of the 2D equilibrium solution

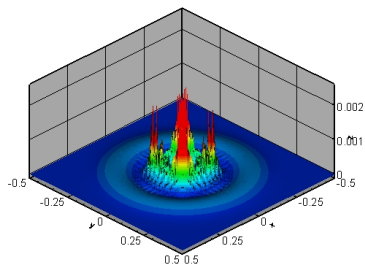
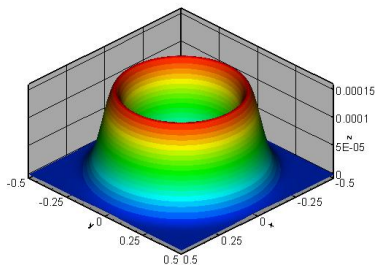


Figure: The 3D views of the velocity $(\sqrt{u^2 + v^2})$. Left: well-balanced methods; Right: non-well-balanced methods.

Structure preserving methods

Structure preserving methods

- Numerical partial differential equations (PDEs): Compute numerical approximation to the solutions of PDEs.
- Exact solutions of PDEs satisfy many continuum properties. Numerical solutions satisfy these properties “approximately”, not exactly.
- **Structure/Feature Preserving methods:**
Preserve the structure or other fundamental continuum property of the underlying problems **in the discrete level**.

Goal:

(Hopefully) produce a more accurate numerical approximation than with general-purpose methods, on relatively coarse meshes.

Examples of structure preserving methods for PDEs

- Mass conservation methods for conservation laws
- Energy conserving, Hamiltonian conserving methods
- Angular momentum, vorticity preserving methods
- Bound preserving, positivity preserving methods
- Symmetry preserving methods
- Globally divergence free methods
- Entropy stable, entropy consistent methods to satisfy the entropy condition
- Asymptotic preserving methods to preserve the asymptotic limit
- Well-balanced methods to preserve the equilibrium state
- ...

The main objective

Develop high order accurate **structure-preserving** discontinuous Galerkin schemes for the hyperbolic balance laws, including the shallow water equations and Euler equations with source terms, which have the key advantage

- High order accuracy;
- Well-balanced for the steady state solutions;
- Positivity-preserving;
- Entropy stable;
- Good resolution for smooth and discontinuous solutions.

1: We expect well-balanced methods to be efficient for **time dependent problems, which are small perturbation of the steady state solutions.**

2: Discontinuous Galerkin methods are presented in this talk, and most of the work have been extended to high order finite difference/finite volume WENO methods.

Recent paper: Veiga, Abgrall, Teyssier (2018), Capturing near-equilibrium solutions: a comparison between high-order discontinuous Galerkin methods and well-balanced schemes

Euler equations with a gravitational potential

Euler equations with a source term due to the static gravitational field:

$$\begin{aligned}\rho_t + \nabla \cdot (\rho \mathbf{u}) &= 0, \\ (\rho \mathbf{u})_t + \nabla \cdot (\rho \mathbf{u} \otimes \mathbf{u} + p \mathbf{I}_d) &= -\rho \nabla \phi, \\ E_t + \nabla \cdot ((E + p) \mathbf{u}) &= -\rho \mathbf{u} \cdot \nabla \phi,\end{aligned}$$

- ρ : fluid density; \mathbf{u} : velocity; p : pressure;
 $E = \frac{1}{2} \rho u^2 + p/(\gamma - 1)$: non-gravitational energy.
- $\phi = \phi(\mathbf{x})$: time independent gravitational potential.
A simple example is: $\phi_z = g$.
- The hydrostatic balance with a zero velocity:

$$\rho = \rho(x), \quad u = 0, \quad \nabla p = -\rho \nabla \phi,$$

where the flux produced by the pressure balances the gravitational source.

Motivation and existing approaches

- Motivation: core-collapse supernova simulation

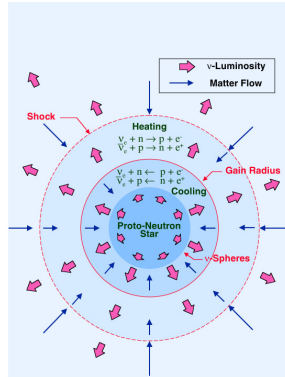
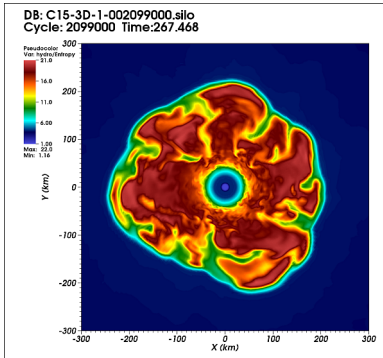


Figure: Image credit: Left: Endeve, Mezzacappa et al. (ORNL); Right: TeraScale Supernova Initiative.

- Many astrophysical problems involve the hydrodynamical evolution in a gravitational field. It is essential to correctly capture the effect of gravitational force in the simulations.

Motivation and existing approaches

- Other applications:
 - ① Stellar “evolution”: Stars evolve mostly quietly, very close to a hydrostatic state.
 - ② Waves in stellar atmospheres: The wave amplitude may be much smaller when compared to the stratification from gravity...
 - ③ Atmospheric flows: Atmospheric motions happen on a hydrostatic background.
- **Improper treatment of the gravitational force** can introduce large spurious oscillations, unless the grid is extremely refined.

Motivation and existing approaches

- Some attempts in designing well-balanced methods for the Euler equations.

LeVeque and Bale 1998

Botta, Klein, Langenberg and Lützenkirchen 2004

Xu and his collaborators 2007, 2010, 2011

Xing, Shu, Li, 2013, 2015, 2016, 2018

Käppeli and Mishra 2014, 2016

Chandrashekar, Klingenberg, Puppo et. al. 2015, 2017, 2018

Chertock, Cui, Kurganovz, Özcan and Tadmor 2018

Chen, Noelle 2018

Veiga, Abgrall, Teysier 2018

...

Steady state solutions

- The hydrostatic balance with a zero velocity:

$$\rho = \rho(x), \quad u = 0, \quad p_x = -\rho\phi_x,$$

where the flux produced by the pressure balances the gravitational source. Two important special steady state are the **constant entropy (isentropic/polytropic)** and **constant temperature (isothermal)** hydrostatic equilibrium states

- **Isothermal equilibrium:** For an ideal gas, we have $p = \rho RT$. The equilibrium (with constant temperature T_0) becomes

$$\rho = \rho_0 \exp\left(-\frac{\phi}{RT_0}\right), \quad u = 0, \quad p = RT_0\rho = p_0 \exp\left(-\frac{\phi}{RT_0}\right).$$

A special case with a linear gravitational potential field: $\phi_x = g$ is:

$$\rho = \rho_0 \exp(-g\rho_0 x/p_0), \quad \mathbf{u} = 0, \quad p = p_0 \exp(-g\rho_0 x/p_0).$$

Steady state solutions

- **Polytropic equilibrium:**

$$p = K\rho^\gamma,$$

which will lead to the form of

$$\rho = \left(\frac{\gamma - 1}{K\gamma} (C - \phi) \right)^{\frac{1}{\gamma-1}}, \quad \mathbf{u} = 0, \quad p = \frac{1}{K^{\frac{1}{\gamma-1}}} \left(\frac{\gamma - 1}{\gamma} (C - \phi) \right)^{\frac{\gamma}{\gamma-1}},$$

or equivalently,

$$h + \phi = \text{const},$$

where $h = e + p/\rho$ is the specific enthalpy and e is the specific internal energy.

A special case with a linear gravitational potential field: $\phi_x = g$ is:

$$p = p_0^{\frac{1}{\gamma-1}} \left(p_0 - \frac{\gamma - 1}{\gamma} g \rho_0 x \right)^{\frac{\gamma}{\gamma-1}}, \quad u = 0, \quad \rho = \rho_0 \left(\frac{p}{p_0} \right)^{\frac{1}{\gamma}}.$$

First and second order finite volume well-balanced methods for polytropic equilibrium are designed by Käppeli and Mishra (2014).

Key idea

- Discretize the source terms using an approximation consistent with that of approximating the flux derivative terms.
- This idea has been used to design well-balanced methods for the shallow-water equations by us.
- The simple steady state

$$\rho = c \exp(-gx), \quad u = 0, \quad p = c \exp(-gx),$$

with $\phi_x = g$ will be used as an example to illustrate the idea.

Equivalent form

- Rewrite the equations as

$$\rho_t + (\rho u)_x = 0$$

$$(\rho u)_t + (\rho u^2 + p)_x = \frac{\rho}{\exp(-gx)} (\exp(-gx))_x$$

$$E_t + ((E + p)u)_x = -\rho u g,$$

Purpose: introduce the derivative term in the source term, which can be treated in the similar way as the flux term.

- Denote them by

$$U_t + F(U)_x = S(U, \phi).$$

Semi-discrete DG scheme

$$U_t + F(U)_x = S(U, \phi).$$

- The semi-discrete DG scheme

$$\int_{I_j} (U_h)_t v dx - \int_{I_j} F(U_h) v_x dx + \hat{F}_{j+\frac{1}{2}} v(x_{j+\frac{1}{2}}^-) - \hat{F}_{j-\frac{1}{2}} v(x_{j-\frac{1}{2}}^+) = \int_{I_j} S v dx,$$

where

$$\hat{F}_{j+\frac{1}{2}} = f(U_h(x_{j+\frac{1}{2}}^-, t), U_h(x_{j+\frac{1}{2}}^+, t)),$$

and $f(a_1, a_2)$ is a numerical flux.

- Lax-Friedrichs flux:

$$f(a_1, a_2) = \frac{1}{2}(F(a_1) + F(a_2) - \alpha(a_2 - a_1)).$$

Well-balanced source term approximation

- We first decompose the integral of the source term in the second equation as

$$\begin{aligned}\int_{I_j} S_2 v dx &= \int_{I_j} \rho \exp(gx) (\exp(-gx))_x v dx = \int_{I_j} \frac{\rho}{b} b_x v dx \\ &= \frac{\rho(x_j)}{b(x_j)} \left(b(x_{j+\frac{1}{2}}^-) v(x_{j+\frac{1}{2}}^-) - b(x_{j-\frac{1}{2}}^+) v(x_{j-\frac{1}{2}}^+) - \int_{I_j} b v_x dx \right) + \int_{I_j} \left(\frac{\rho}{b} - \frac{\rho(x_j)}{b(x_j)} \right) b_x v dx,\end{aligned}$$

where $b(x) = \exp(-gx)$.

- Let $b_h(x)$ be the projection of $b(x)$ into V_h^k , approximate the integral by:

$$\begin{aligned}\int_{I_j} S_2 v dx &\approx \int_{I_j} \left(\frac{\rho_h}{b_h} - \frac{\rho_h(x_j)}{b_h(x_j)} \right) (b_h)_x v dx \\ &\quad + \frac{\rho_h(x_j)}{b_h(x_j)} \left(\{b_h\}(x_{j+\frac{1}{2}}) v(x_{j+\frac{1}{2}}^-) - \{b_h\}(x_{j-\frac{1}{2}}) v(x_{j-\frac{1}{2}}^+) - \int_{I_j} b_h v_x dx \right).\end{aligned}$$

- Use quadrature rule to approximate the source term in the third equation

$$\int_{I_j} S_3 v dx \approx \int_{I_j} -(\rho u)_h g v dx.$$

Well-balanced fix to the numerical flux

- Lax-Friedrichs flux:

$$f(a_1, a_2) = \frac{1}{2}(F(a_1) + F(a_2) - \alpha(a_2 - a_1)).$$

$\alpha(a_2 - a_1)$ contributes to the numerical viscosity term, but may **destroy the well-balanced property at the steady state**.

- Well-balanced modification:

$$\hat{F}_{j+1/2} = \frac{1}{2} \left[F \left(U_h(x_{j+1/2}^-) \right) + F \left(U_h(x_{j+1/2}^+) \right) - \alpha' \left(\frac{U_h(x_{j+1/2}^+)}{b_h(x_{j+1/2}^+)} - \frac{U_h(x_{j+1/2}^-)}{b_h(x_{j+1/2}^-)} \right) \right].$$

To maintain enough artificial numerical viscosity:

$$\alpha' = \alpha \max_x b_h(x),$$

At the steady state, the numerical flux reduces to

$$\hat{f}_{j+\frac{1}{2}} = \frac{1}{2} \left[f \left(U(x_{j+1/2}^-) \right) + f \left(U(x_{j+1/2}^+) \right) \right].$$

Main result

Proposition: For the Euler equations with the linear gravitational potential field, the semi-discrete DG methods mentioned above can maintain the **original high order accuracy** and are **well-balanced** for the steady state solution.

Proof: At the steady state, we have

$$\rho_h = cb_h, \quad u = 0, \quad p_h = cb_h.$$

For the momentum equation, the source term approximation becomes

$$\int_{I_j} S_2 v dx \approx c \left(\{b_h\}(x_{j+\frac{1}{2}})v(x_{j+\frac{1}{2}}^-) - \{b_h\}(x_{j-\frac{1}{2}})v(x_{j-\frac{1}{2}}^+) - \int_{I_j} b_h v_x dx \right).$$

Since $u = 0$, the flux term $F_2 = \rho u^2 + p$ reduces to $p = cb$. Its numerical approximation takes the form of

$$\begin{aligned} & \hat{F}_2(x_{j+\frac{1}{2}})v(x_{j+\frac{1}{2}}^-) - \hat{F}_2(x_{j-\frac{1}{2}})v(x_{j-\frac{1}{2}}^+) - \int_{I_j} F_2 v_x dx \\ &= c\{b_h\}(x_{j+\frac{1}{2}})v(x_{j+\frac{1}{2}}^-) - c\{b_h\}(x_{j-\frac{1}{2}})v(x_{j-\frac{1}{2}}^+) - \int_{I_j} cb_h v_x dx. \end{aligned}$$

General steady state

$$\rho = \rho_0 \exp\left(-\frac{\phi}{RT_0}\right), \quad u = 0, \quad p = RT_0\rho = RT_0\rho_0 \exp\left(-\frac{\phi}{RT_0}\right).$$

- We first **rewrite the equations**:

$$\rho_t + (\rho u)_x = 0,$$

$$(\rho u)_t + (\rho u^2 + p)_x = RT_0\rho \exp\left(\frac{\phi}{RT_0}\right) \left(\exp\left(-\frac{\phi}{RT_0}\right)\right)_x,$$

$$E_t + ((E + p)u)_x = -\rho u g,$$

- **Well-balanced source term approximation**:

$$\begin{aligned} \int_{I_j} S_2 v dx &\approx \int_{I_j} RT_0 \left(\frac{\rho_h}{d_h} - \frac{\rho_h(x_j)}{d_h(x_j)} \right) (d_h)_x v dx \\ &+ RT_0 \frac{\rho_h(x_j)}{d_h(x_j)} \left(\{d_h\}(x_{j+\frac{1}{2}}) v(x_{j+\frac{1}{2}}^-) - \{d_h\}(x_{j-\frac{1}{2}}) v(x_{j-\frac{1}{2}}^+) - \int_{I_j} d_h v_x dx \right), \end{aligned}$$

where $d(x) = \exp\left(-\frac{\phi}{RT_0}\right)$.

- **Well-balanced fix to the numerical flux**.

Multi-dimensional Euler equations

- The Euler equations with a static gravitational field are

$$\rho_t + \nabla \cdot (\rho \mathbf{u}) = 0,$$

$$(\rho \mathbf{u})_t + \nabla \cdot (\rho \mathbf{u} \otimes \mathbf{u} + p \mathbf{I}_d) = -\rho \nabla \phi,$$

$$E_t + \nabla \cdot ((E + p) \mathbf{u}) = -\rho \mathbf{u} \cdot \nabla \phi,$$

- Hydrostatic balance:

$$\rho = \rho_0 \exp\left(-\frac{\phi}{RT}\right), \quad \mathbf{u} = 0, \quad p = RT\rho = RT\rho_0 \exp\left(-\frac{\phi}{RT}\right),$$

with constant temperature T .

- A special case is:

$$\rho = \rho_0 \exp(-\rho_0(\mathbf{g} \cdot \mathbf{x})/p_0), \quad u = v = 0, \quad p = p_0 \exp(-\rho_0(\mathbf{g} \cdot \mathbf{x})/p_0),$$

with a linear gravitational potential field: $\phi(\mathbf{x}) = \mathbf{g} \cdot \mathbf{x}$.

Well-balanced methods

$$\rho = \rho_0 \exp\left(-\frac{\phi}{RT}\right), \quad \mathbf{u} = 0, \quad p = RT\rho = RT\rho_0 \exp\left(-\frac{\phi}{RT}\right).$$

- We first **rewrite the source term**:

$$-\rho \nabla \phi = RT\rho \exp\left(\frac{\phi}{RT}\right) \nabla \left(\exp\left(-\frac{\phi}{RT}\right)\right) = \frac{RT\rho}{d} \nabla d.$$

- **Well-balanced source term approximation**:

$$\begin{aligned} \int_K S_2 w \, dx &\approx \int_K RT \left(\frac{\rho_h}{d_h} - \frac{\rho_h(\mathbf{x}_K^0)}{d_h(\mathbf{x}_K^0)} \right) \nabla d_h w \, dx \\ &\quad + RT \frac{\rho_h(\mathbf{x}_K^0)}{d_h(\mathbf{x}_K^0)} \left(\sum_{i=1}^m \int_{e_K^i} \{d_h(\mathbf{x})\} \nu_K^i w \, ds - \int_K d_h \nabla w \, dx \right), \end{aligned}$$

where $d(x) = \exp\left(-\frac{\phi}{RT}\right)$.

- **Well-balanced fix to the numerical flux**.

The same technique can be extended to the polytropic equilibrium state, and other given equilibrium state.

Well-balanced approach via hydrostatic reconstruction

Well-balanced methods for the polytropic balance

Key idea:

Decompose the solution into equilibrium and non-equilibrium parts, and treat them differently.

Components:

- Recovery of well-balanced states;
- Decomposition of the solutions into equilibrium and non-equilibrium parts;
- Numerical fluxes via hydrostatic reconstruction;
- Novel source term approximation.

Use 1D Euler equation as example to demonstrate the algorithm.

Recovery of well-balanced states

Suppose $U(x, t = 0) = U^0(x)$ are in perfect equilibrium, i.e.,

$$u^0(x) = 0, \quad h(x) + \phi(x) = \text{const } C.$$

- Initial condition for DG methods is the projection of these to $V_{\Delta x}$.
- Usually L^2 projection is used. But it is **difficult to retrieve the constant C** from the projected initial condition.
- In our previous FV work for the shallow water equations, we define it as a solution of a nonlinear equation and solve it using Newton's iteration.

Recovery of well-balanced states

Suppose $U(x, t = 0) = U^0(x)$ are in perfect equilibrium, i.e.,

$$u^0(x) = 0, \quad h(x) + \phi(x) = \text{const } C.$$

- DG methods are more flexible.

We define **Projection** $P_h^+ \omega$ as a projection of $\omega(x)$ into $V_{\Delta x}$:

$$\int_{I_j} P_h^+ \omega v dx = \int_{I_j} \omega v dx,$$

for any $v \in P^{k-1}$ on I_j , and

$$P_h^+ \omega(x_{j-\frac{1}{2}}^+) = \omega(x_{j-\frac{1}{2}}) \quad \text{at the left boundary } x_{j-\frac{1}{2}}.$$

- We can verify this projection is **optimal**, i.e., $\|P_h^+ U(x) - U(x)\| = O(h^{k+1})$, plus we have

$$h(p_h(x_{j-\frac{1}{2}}), \rho_h(x_{j-\frac{1}{2}})) + \phi_h(x_{j-\frac{1}{2}}) = \text{const } C,$$

where $U_h(x) = P_h^+ U(x)$, $\rho_h(x) = P_h^+ \rho(x)$ etc.

Decomposition into equilibrium and non-equilibrium parts

- **Key idea:** decompose U_h into the sum of a reference equilibrium state U_h^e and the remaining part U_h^r .

- $U_h^e(x)$?

Let $h^e(x) = h(p_h(x_{j-\frac{1}{2}}), \rho_h(x_{j-\frac{1}{2}})) + \phi_h(x_{j-\frac{1}{2}}) - \phi(x)$. Recover $\rho^e(x)$ and $p^e(x)$ from $h^e(x)$. For the ideal gas law, we have the polytropic form

$$\rho^e(x) = \left(\frac{1}{K} \frac{\gamma-1}{\gamma} h^e(x) \right)^{\frac{1}{\gamma-1}}, \quad u^e(x) = 0, \quad p^e(x) = \left(\frac{1}{K} \right)^{\frac{1}{\gamma-1}} \left(\frac{\gamma-1}{\gamma} h^e(x) \right)^{\frac{\gamma}{\gamma-1}}.$$

We can compute $U^e(x)$, and define $U_h^e(x) = P_h^+ U^e(x)$.

- $U_h^r = U_h(x) - U_h^e(x)$.

Note that both U_h^e and U_h^r are piecewise polynomials.

- At the polytropic steady state, $U_h^r(x) = 0$.

Well-balanced fluxes (Hydrostatic reconstruction)

- The hydrostatic reconstructed cell boundary values are defined by:

$$U_{j+\frac{1}{2}}^{*,\pm} = U^e \left(h(p_h(x_j), \rho_h(x_j)) + \phi_h(x_j) - \max(\phi_{h,j+\frac{1}{2}}^{\pm}) \right) + (U_h^r)_{j+\frac{1}{2}}^{\pm},$$

In the case of polytropic equilibrium, $U_{j+\frac{1}{2}}^{*,+} = U_{j+\frac{1}{2}}^{*,-}$.

- The left and right fluxes $\widehat{f}_{j+\frac{1}{2}}^l$ and $\widehat{f}_{j-\frac{1}{2}}^r$ are given by:

$$\begin{aligned}\widehat{f}_{j+\frac{1}{2}}^l &= F(U_{j+\frac{1}{2}}^{*,-}, U_{j+\frac{1}{2}}^{*,+}) + f(U_{j+\frac{1}{2}}^-) - f(U_{j+\frac{1}{2}}^{*,-}), \\ \widehat{f}_{j-\frac{1}{2}}^r &= F(U_{j-\frac{1}{2}}^{*,-}, U_{j-\frac{1}{2}}^{*,+}) + f(U_{j-\frac{1}{2}}^+) - f(U_{j-\frac{1}{2}}^{*,+}).\end{aligned}$$

Source term approximation

- For $-\int (\rho u)_h (\phi_h)_x v dx$, we apply the Gaussian quadrature rule directly.
- $-\rho_h (\phi_h)_x$ is linear with respect to ρ_h , we have

$$-\int \rho_h (\phi_h)_x v dx = -\int \rho_h^e (\phi_h)_x v dx - \int \rho_h^r (\phi_h)_x v dx,$$

which can be approximated by:

$$-\int \rho_h (\phi_h)_x v dx \approx p_{h,j+\frac{1}{2}}^{e,-} v(x_{j+\frac{1}{2}}^-) - p_{h,j-\frac{1}{2}}^{e,+} v(x_{j-\frac{1}{2}}^+) - \int_{I_j} p_h^e v_x dx - \int_{I_j} \rho_h^r (\phi_h)_x v dx,$$

using the fact that U_h^e is the equilibrium state.

Well-balanced methods for polytropic balance

$$\int_{I_j} \partial_t U^n v dx - \int_{I_j} f(U^n) \partial_x v dx + \widehat{f}_{j+\frac{1}{2}}^l v(x_{j+\frac{1}{2}}^-) - \widehat{f}_{j-\frac{1}{2}}^r v(x_{j-\frac{1}{2}}^+) = \int_{I_j} s(h^n, b) v dx,$$

Proposition: The DG schemes described above **maintain polytropic equilibrium exactly**.

Remarks

- If there is no gravitation field, i.e., $\phi_x = 0$, our well-balanced DG methods become the traditional DG methods.
- The first order version of our well-balanced methods reduces to the method in (Käppeli and Mishra, JCP 2014).

The same technique can be extended to the isothermal equilibrium state (Li-X, JCP 2018).

Multi-dimensional Euler equations on unstructured meshes

The same four components: (details skipped)

- Recovery of well-balanced states;
- Decomposition of the solutions into equilibrium and non-equilibrium parts;
- Numerical fluxes via hydrostatic reconstruction;
- Novel source term approximation;

Numerical results

- The third order finite element DG schemes are implemented, for the flux and the source terms.
- Time discretization is by the third order TVD Runge-Kutta method:

$$\begin{aligned}U^{(1)} &= U^n + \Delta t \mathcal{F}(U^n) \\U^{(2)} &= \frac{3}{4}U^n + \frac{1}{4} \left(U^{(1)} + \Delta t \mathcal{F}(U^{(1)}) \right) \\U^{n+1} &= \frac{1}{3}U^n + \frac{2}{3} \left(U^{(2)} + \Delta t \mathcal{F}(U^{(2)}) \right),\end{aligned}$$

where $\mathcal{F}(U)$ is the spatial operator.

- The CFL number is taken as 0.18.

One dimensional polytropic equilibrium solution

- The gravitational force, with $g = \phi_x = 1$, acts in the negative x direction.
- Consider a polytropic equilibrium solution

$$\rho(x) = \left(\rho_0^{\gamma-1} - \frac{1}{K_0} \frac{\gamma-1}{\gamma} g x \right)^{\frac{1}{\gamma-1}}, \quad u(x) = 0, \quad p(x) = K_0 \rho(x)^\gamma,$$

in the domain $[0, 2]$, with $\gamma = 5/3$, $\rho_0 = 1$, $p_0 = 1$ and $K_0 = p_0/\rho_0^\gamma$.

Table: L^1 errors for different precisions.

N	Precision	ρ	ρu	E
100	Single	1.01E-6	1.48E-7	8.27E-7
	Double	1.33E-15	1.55E-16	8.75E-16
200	Single	4.53E-6	5.24E-7	2.83E-7
	Double	3.34E-15	5.10E-15	2.67E-16

Perturbation of the equilibrium solution

Impose a small perturbation to the velocity state at the bottom

$$u(0, t) = 10^{-6} \sin(4\pi t)$$

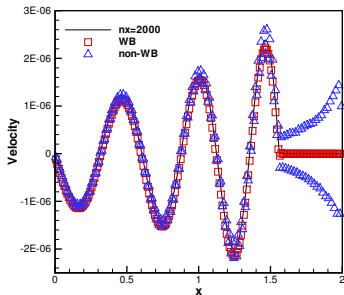
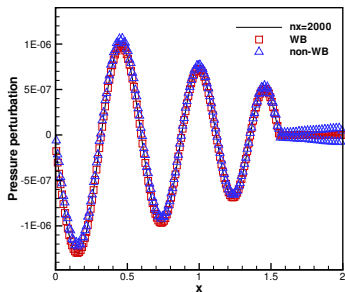


Figure: The pressure perturbations (left) and velocity (right) of a hydrostatic solution with small perturbation. The results of the well-balanced method vs. non-well-balanced method.

Perturbation of the equilibrium solution

Impose a large perturbation to the velocity state at the bottom

$$u(0, t) = 10^{-1} \sin(4\pi t)$$

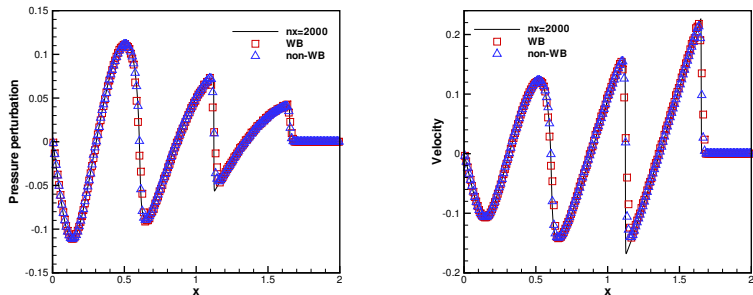


Figure: The pressure perturbations (left) and velocity (right) of a hydrostatic solution with large perturbation. The results of the well-balanced method vs. non-well-balanced method.

One dimensional isothermal equilibrium solution

- The gravitational force, with $g = \phi_x = 1$, acts in the negative x direction.
- Consider an isothermal equilibrium solution

$$\rho_0(x) = p_0(x) = \exp(-x), \quad \text{and} \quad u_0(x) = 0.$$

in the domain $[0, 1]$.

Table: L^1 errors for different precisions.

N	Precision	ρ	ρu	E
100	Single	2.38E-7	2.23E-7	4.55E-7
	Double	1.76E-15	1.77E-15	1.24E-15
200	Single	3.13E-7	2.34E-7	4.31E-7
	Double	2.99E-15	1.61E-15	1.84E-15

Perturbation of the equilibrium solution

Impose a small perturbation to the initial pressure state

$$p(x, t = 0) = p_0(x) + \eta \exp(-100(x - 0.5)^2),$$

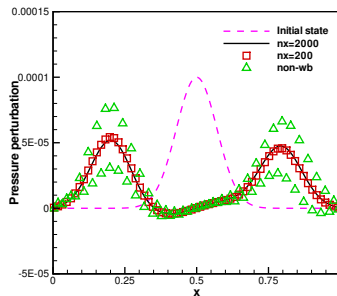
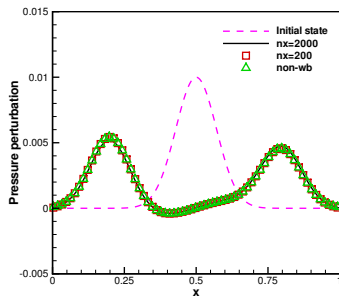


Figure: The pressure perturbation of a hydrostatic solution. The results of the well-balanced method vs. non-well-balanced method. Left: $\eta = 0.01$; Right: $\eta = 0.0001$.

One dimensional gas falling into a fixed external potential

- The gravitational potential has the form of a sine wave,

$$\phi(x) = -\phi_0 \frac{L}{2\pi} \sin \frac{2\pi x}{L},$$

where L is the computational domain length and ϕ_0 is the amplitude.

- Consider an isothermal equilibrium solution

$$\rho = \rho_0 \exp\left(-\frac{\phi}{RT}\right), \quad u = 0, \quad p = RT\rho_0 \exp\left(-\frac{\phi}{RT}\right),$$

with a constant temperature T .

- Add a small perturbation to the steady state:

$$\begin{aligned} \rho &= \rho_0 \exp\left(-\frac{\phi}{RT}\right), \quad u = 0, \\ p &= RT\rho_0 \exp\left(-\frac{\phi}{RT}\right) + 0.001 \exp(-10(x - 32)^2). \end{aligned}$$

- We run the simulation with 64 uniform cells for 1,000,000 time steps.

One dimensional gas falling into a fixed external potential

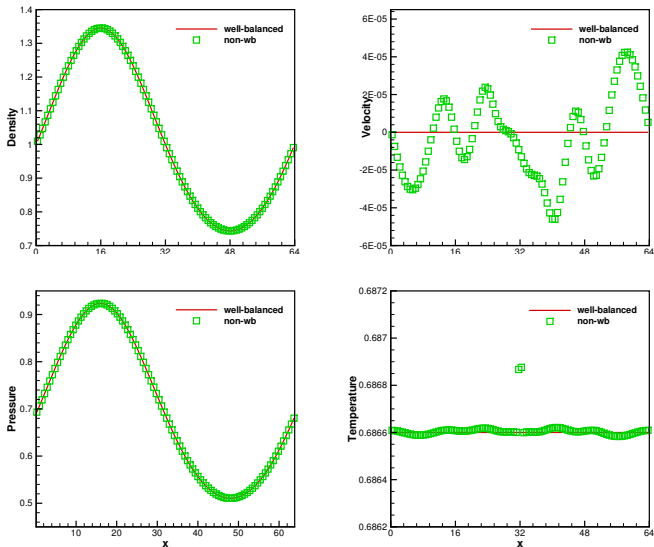


Figure: The numerical solutions of well-balanced method (solid line) and non-well-balanced method (square box, denoted by non-wb).

Two dimensional accuracy test

- Consider a linear gravitational field $\phi_x = \phi_y = 1$, in a computational domain $[0, 2] \times [0, 2]$.
- A time dependent exact solution

$$\rho(x, y, t) = 1 + 0.2 \sin(\pi(x + y - t(u_0 + v_0))),$$

$$u(x, y, t) = u_0, \quad v(x, y, t) = v_0,$$

$$p(x, y, t) = t(u_0 + v_0) - x - y + 0.2\pi \cos(\pi(x + y - t(u_0 + v_0))).$$

- The exact solutions are used as the boundary condition. We compute up to $t = 0.1$.

Two dimensional accuracy test

Table: L^1 errors and numerical orders of accuracy for the example (the error of ρv is similar to ρu and is not listed here).

Cells	ρ		ρu		E	
	L^1 error	Order	L^1 error	Order	L^1 error	Order
8×8	1.20E-04		1.09E-04		2.84E-04	
16×16	1.19E-05	3.33	1.13E-05	3.27	3.18E-05	3.16
32×32	1.14E-06	3.39	1.17E-06	3.27	3.61E-06	3.14
64×64	1.35E-07	3.07	1.58E-07	2.89	4.10E-07	3.14
128×128	1.80E-08	2.91	2.15E-08	2.88	4.78E-08	3.10
256×256	2.41E-09	2.90	2.94E-09	2.87	5.93E-09	3.01

Two dimensional polytrope

- An adiabatic gaseous sphere held together by self-gravitation, modeled by the hydrostatic equilibrium

$$\frac{dp}{dr} = -\rho \frac{d\phi}{dr},$$

and Poisson's equation with $r = \sqrt{x^2 + y^2}$

$$\frac{1}{r^2} \frac{d}{dr} \left(r^2 \frac{d\phi}{dr} \right) = 4\pi g \rho.$$

- Use the polytropic relation $p = K\rho^\gamma$, assume $\gamma = 2$ to obtain solutions:

$$\rho(r) = \rho_c \frac{\sin(\alpha r)}{\alpha r}, \quad p(r) = K\rho(r)^2, \quad (1)$$

with $\alpha = \sqrt{\frac{4\pi g}{2K}}$, and the gravitational potential

$$\phi(r) = -2K\rho_c \frac{\sin(\alpha r)}{\alpha r}. \quad (2)$$

The parameters $K = g = \rho_c = 1$ are used.

Small perturbation of the 2D polytrope

Consider a small Gaussian hump perturbations to the initial pressure state

$$p(r) = K\rho(r)^2 + A \exp(-100r^2),$$

where A is taken as 10^{-3} .

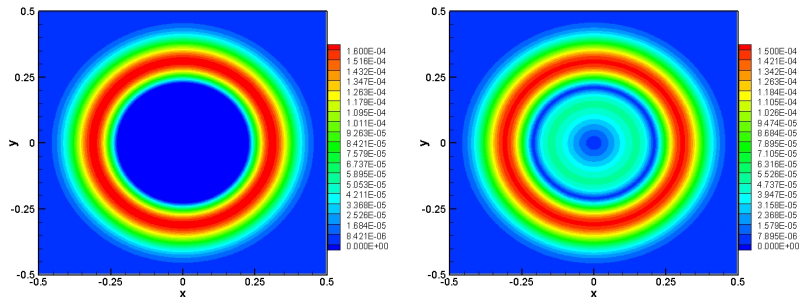


Figure: Well-balanced methods: The contours of the pressure and velocity perturbation of a two dimensional hydrostatic solution with 100×100 cells at $t = 0.2$. Left: pressure p . Right: velocity $\sqrt{u^2 + v^2}$.

Small perturbation of the 2D polytrope

Consider a small Gaussian hump perturbations to the initial pressure state

$$p(r) = K\rho(r)^2 + A \exp(-100r^2),$$

where A is taken as 10^{-3} .

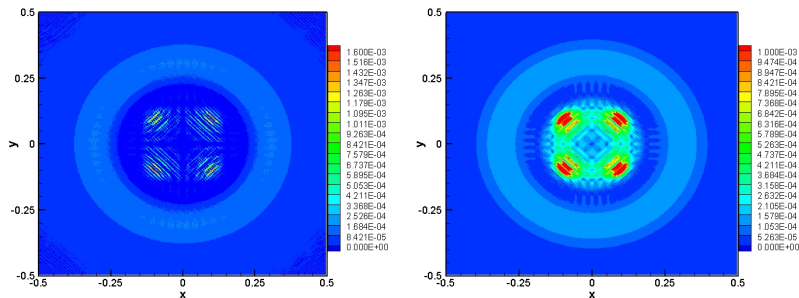


Figure: Non-well-balanced methods: The contours of the pressure and velocity perturbation of a two dimensional hydrostatic solution with 100×100 cells at $t = 0.2$. Left: pressure p . Right: velocity $\sqrt{u^2 + v^2}$. Notice the different contour range.

Small perturbation of the 2D equilibrium solution

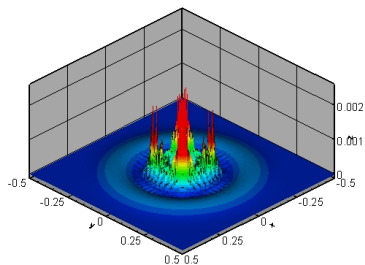
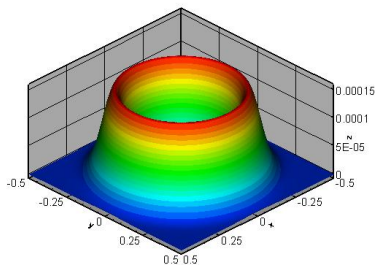


Figure: The 3D views of the velocity $(\sqrt{u^2 + v^2})$. Left: well-balanced methods; Right: non-well-balanced methods.

Two-dimensional Explosion Problem

- Linear gravitational field with $\phi_x = 0$, $\phi_y = g = 0.118$, an ideal gas ($\gamma = 1.4$)
- On the domain $[0, 3] \times [0, 3]$, initial conditions

$$\rho(x, y, t = 0) = 1,$$

$$u(x, y, t = 0) = 0,$$

$$v(x, y, t = 0) = 0,$$

$$p(x, y, t = 0) = 1 - gy + \begin{cases} 0.005, & \text{if } (x - 1.5)^2 + (y - 1.5)^2 < 0.01, \\ 0, & \text{otherwise.} \end{cases}$$

- This test can also be viewed as a small perturbation of the steady state solution. But the underline steady state **does not have the form of polytropic nor isothermal balance.**

Two-dimensional Explosion Problem

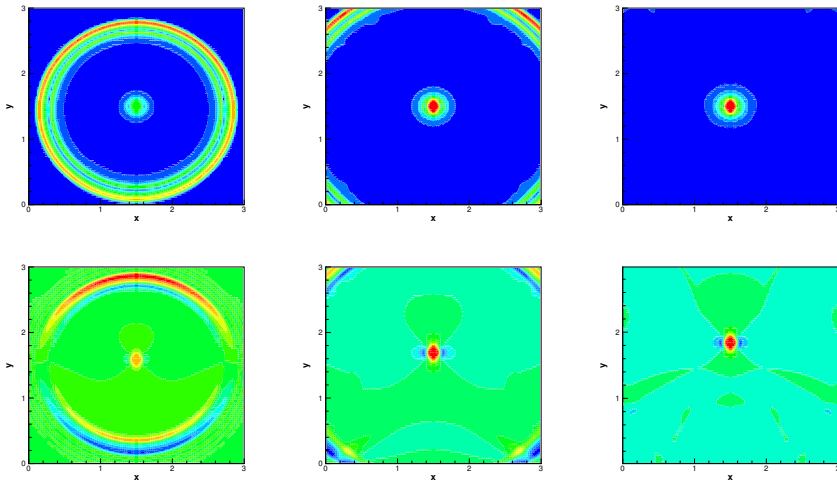


Figure: Velocity $\sqrt{u^2 + v^2}$ at times $t = 1.2$ (left), $t = 1.8$ (middle) and $t = 2.4$ (right). Top: well-balanced. Bottom: non-well-balanced. Ten uniformly spaced contour lines from 0.2829 to 0.2838.

Positivity preserving (PP) methods

Existing work on PP DG methods for Euler equations

$$\begin{aligned}\rho_t + \nabla \cdot (\rho \mathbf{u}) &= 0, \\ (\rho \mathbf{u})_t + \nabla \cdot (\rho \mathbf{u} \otimes \mathbf{u} + p \mathbf{I}_d) &= -\rho \nabla \phi, \\ E_t + \nabla \cdot ((E + p) \mathbf{u}) &= -\rho \mathbf{u} \cdot \nabla \phi,\end{aligned}$$

- Density ρ and internal energy e should stay non-negative
- Many existing works available on PP methods for Euler equations, here we focus on [Zhang-Shu JCP 2011](#) for Euler equations with source terms
- Define the set of physically admissible states

$$G := \left\{ \mathbf{U} = (\rho, \mathbf{m}, E)^\top : \rho > 0, \mathcal{E}(\mathbf{U}) := \rho E - \frac{|\mathbf{m}|^2}{2} > 0 \right\},$$

G is a convex set.

PP methods for Euler equations by Zhang-Shu JCP 2011

(Without source term) to achieve **high order & positivity**

$$\boxed{\mathbf{U}_h^n(x) \in G} \xrightarrow[\text{step 1}]{\text{DG update}} \boxed{\mathbf{U}_h^{n+1}(x) \text{ with } \bar{\mathbf{U}}_{h,j}^{n+1} \in G} \xrightarrow[\text{step 2}]{\text{limiter}} \boxed{\mathbf{U}_h^{n+1}(x) \in G}$$

- Step 1: **proven analytically** under the CFL condition $\alpha \Delta t / \Delta x \leq \hat{w}_1$
- Step 2: obtained via a **simple PP limiter** on density ρ

$$\tilde{\rho}_j^n(x) = \theta (\rho_j^n(x) - \bar{\rho}_j^n) + \bar{\rho}_j^n, \quad \theta = \min \left\{ 1, \frac{\bar{\rho}_j^n}{\bar{\rho}_j^n - m_j} \right\},$$

with

$$m_j = \min_{x \in I_j} \rho_j^n(x).$$

Similar limiter can be applied on the internal energy e (different definition of θ)

This limiter does not affect the high order accuracy and mass conservation.

PP methods for Euler equations by Zhang-Shu JCP 2011

(With source term $s(\mathbf{U}, x)$) to achieve **high order & positivity**

$$\boxed{\mathbf{U}_h^n(x) \in G} \xrightarrow[\text{step 1}]{\text{DG update}} \boxed{\mathbf{U}_h^{n+1}(x) \text{ with } \overline{\mathbf{U}}_{h,j}^{n+1} \in G} \xrightarrow[\text{step 2}]{\text{limiter}} \boxed{\mathbf{U}_h^{n+1}(x) \in G}$$

- Step 1: **proven analytically** under the CFL condition

$$\alpha \Delta t / \Delta x \leq \hat{w}_1 / 2, \quad \text{and} \quad \Delta t \leq A_s(\mathbf{U}_h, x),$$

where $\Delta t \leq A_s(\mathbf{U}_h, x)$ is chosen such that $\mathbf{U} + 2\Delta t s(\mathbf{U}, x) \in G$.

When the gravitational source $-\rho\phi_x$ is considered, the extra CFL condition is:

$$\Delta t \leq \frac{\sqrt{2e}}{\phi_x},$$

- Step 2: SAME PP limiter.

PP well-balanced methods (step 1)

Combining these PP techniques with the proposed well-balanced methods

PP result

Assume that $\bar{\mathbf{U}}_{h,j} \in G$ and $\mathbf{U}_h(\hat{x}_j^{(\nu)}) \in G$, $1 \leq \nu \leq L$, $\forall j$. Then under the CFL-type condition

$$\Delta t \left\{ \frac{\alpha_{j+\frac{1}{2}} \rho_{j+\frac{1}{2}}^{e,\max}}}{\Delta x \hat{w}_1 \rho_h^e(x_{j+\frac{1}{2}}^-)} \left[\frac{\beta_{j+\frac{1}{2}}}{\beta_h(x_{j+\frac{1}{2}}^-)} + \left(\frac{\beta_{j+\frac{1}{2}}}{\beta_h(x_{j+\frac{1}{2}}^-)} - 1 \right) \frac{|u_{j+\frac{1}{2}}^-|^2}{2e_{j+\frac{1}{2}}^-} \right] + a_j^{\max} + \bar{a}_j \right\} \leq 1$$

with $\beta_h = p_h / \rho_h$, $\beta_{j+\frac{1}{2}} = \max(\beta_h(x_{j+\frac{1}{2}}^-), \beta_h(x_{j+\frac{1}{2}}^+))$,

$$a_j^{\max} := \max_{1 \leq \mu \leq N} \left\{ \frac{|(p_h^e)_x(x_j^{(\mu)})|}{\rho_h^e(x_j^{(\mu)}) \sqrt{2e_h(x_j^{(\mu)})}} \right\}, \quad \bar{a}_j := \frac{|p_h^e(x_{j+\frac{1}{2}}^+) - p_h^e(x_{j-\frac{1}{2}}^-)|}{\Delta x (\rho_h^e)_j \sqrt{2\bar{e}_j}},$$

one has

$$\bar{\mathbf{U}}_j + \Delta t \mathbf{L}_j(\mathbf{U}_h) \in G, \quad \forall j.$$

Restrictive CFL condition due to the **modification of the numerical viscosity** in the well-balanced LF flux

Modification of the well-balanced numerical fluxes

The HLLC numerical flux defined by

$$\mathbf{F}^{hllc}(\mathbf{U}_L, \mathbf{U}_R) = \begin{cases} \mathbf{F}(\mathbf{U}_L), & \text{if } 0 \leq S_L, \\ \mathbf{F}_{*L}, & \text{if } S_L \leq 0 \leq S_*, \\ \mathbf{F}_{*R}, & \text{if } S_* \leq 0 \leq S_R, \\ \mathbf{F}(\mathbf{U}_R), & \text{if } 0 \geq S_R, \end{cases}$$

has the following **contact property and positivity-preserving property**:

- For any two states $\mathbf{U}_L = (\rho_L, 0, p/(\gamma - 1))^\top$ and $\mathbf{U}_R = (\rho_R, 0, p/(\gamma - 1))^\top$,

$$\mathbf{F}^{hllc}(\mathbf{U}_L, \mathbf{U}_R) = (0, p, 0)^\top.$$

Shown in [Chandrashekar-Klingenbergl SISC 2015](#)

- Let $\mathcal{R}(x/t, \mathbf{U}_L, \mathbf{U}_R)$ be the approximate HLLC solution of the Riemann problem between the states \mathbf{U}_L and \mathbf{U}_R , Then, $\mathcal{R}(x/t, \mathbf{U}_L, \mathbf{U}_R) \in G$, provided that \mathbf{U}_L and $\mathbf{U}_R \in G$.

Modification of the well-balanced numerical fluxes

Modified well-balanced numerical fluxes:

$$\widehat{\mathbf{F}}_{j+\frac{1}{2}} = \mathbf{F}^{hllc} \left(\frac{p_{j+\frac{1}{2}}^{e,*}}{p_h^e(x_{j+\frac{1}{2}}^-)} \mathbf{U}_{j+\frac{1}{2}}^-, \frac{p_{j+\frac{1}{2}}^{e,*}}{p_h^e(x_{j+\frac{1}{2}}^+)} \mathbf{U}_{j+\frac{1}{2}}^+ \right),$$

where $\mathbf{U}_{j+\frac{1}{2}}^\pm := \mathbf{U}_h(x_{j+\frac{1}{2}}^\pm)$, and $p_{j+\frac{1}{2}}^{e,*} = \max \left\{ p_h^e(x_{j+\frac{1}{2}}^-), p_h^e(x_{j+\frac{1}{2}}^+) \right\}$.

PP result (step 1 only)

Assume that $\bar{\mathbf{U}}_{h,j} \in G$ and $\mathbf{U}_h(\hat{x}_j^{(\nu)}) \in G$, $1 \leq \nu \leq L$, $\forall j$. Then under the CFL-type condition

$$\Delta t \left\{ \frac{2p_{j\pm\frac{1}{2}}^{e,*}}{\Delta x \hat{\omega}_1 p_h^e(x_{j\pm\frac{1}{2}}^\mp)} \alpha_\infty + a_j^{\max} + \bar{a}_j \right\} \leq 1, \quad \forall j,$$

with $\alpha_\infty := \max \alpha(\mathbf{U}_{j\pm\frac{1}{2}}^\pm)$ and

$$a_j^{\max} := \max_{1 \leq \mu \leq N} \left\{ \frac{|(p_h^e)_x(x_j^{(\mu)})|}{\rho_h^e(x_j^{(\mu)}) \sqrt{2e_h(x_j^{(\mu)})}} \right\}, \quad \bar{a}_j := \frac{|p_h^e(x_{j+\frac{1}{2}}^+) - p_h^e(x_{j-\frac{1}{2}}^-)|}{\Delta x (\rho_h^e)_j \sqrt{2\bar{e}_j}},$$

one has

$$\bar{\mathbf{U}}_j + \Delta t \mathbf{L}_j(\mathbf{U}_h) \in G, \quad \forall j.$$

Rarefaction test with low density and low pressure

- A quadratic potential $\phi(x) = \frac{1}{2}x^2$ centered around $x = 0$
- Consider an initial condition

$$\rho(x, 0) = 7, \quad p(x, 0) = 0.2, \quad u(x, 0) = \begin{cases} -1, & x < 0, \\ 1, & x > 0. \end{cases}$$

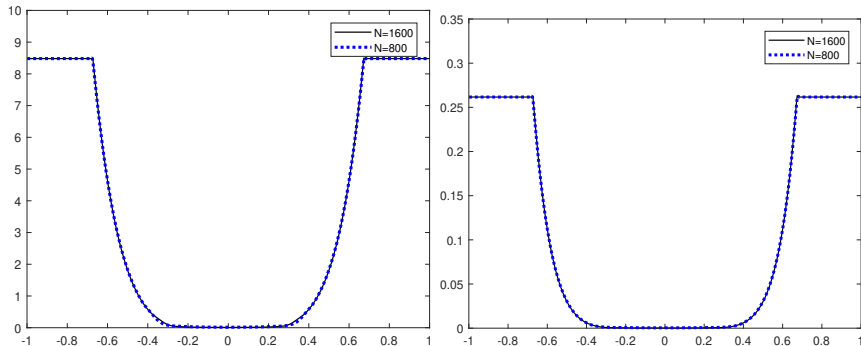


Figure: Density (left) and pressure (right) for the rarefaction test at $t = 0.6$ obtained by the positivity-preserving WB scheme with 800 and 1600 cells.

Leblanc problem in linear gravitational field

A linear potential $\phi(x) = x$ with the initial condition

$$(\rho, u, p)(x, 0) = \begin{cases} (2, 0, 10^9), & x < 5, \\ (10^{-3}, 0, 1), & x > 5. \end{cases}$$

This problem is highly challenging due to the presence of the strong jumps in the initial density and pressure.

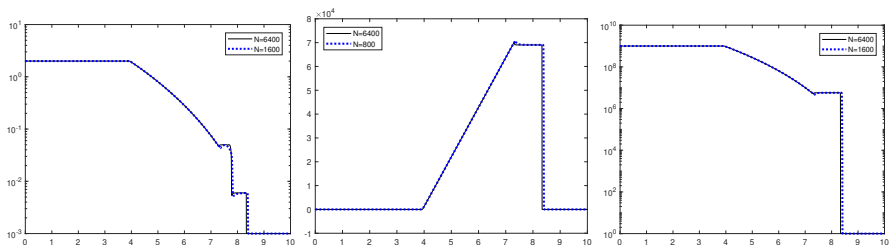


Figure: The log plot of density (left), the velocity (middle) and the log plot of pressure (right) for the extended Leblanc problem at $t = 0.00004$ obtained by the positivity-preserving WB scheme with 1600 and 6400 cells.

Two-dimensional blast problem

The initial data is obtained by adding a huge jump to the pressure term of a polytropic equilibrium.

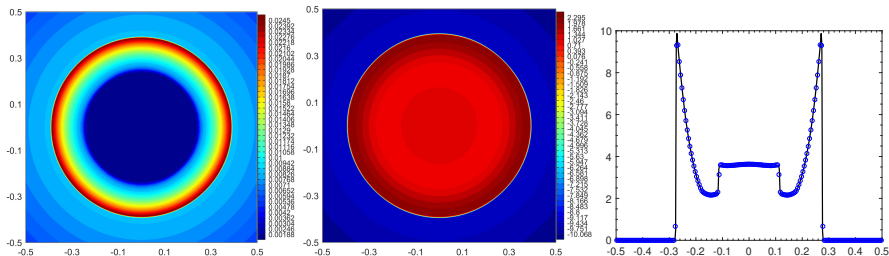


Figure: The contour plots of the density ρ (left) and the pressure logarithm $\log(p)$ (middle) at $t = 0.005$, and the plot of p (right) along the line $y = x$ within the scaled interval $[-0.5, 0.5]$, obtained by the positivity-preserving well-balanced DG scheme with 400×400 cells.

Introduction

Blood flow models have been extensively used to mathematically understand and numerically simulate the **human cardiovascular system**.

History of Arterial Blood Flow Models:

- Euler (1775) derived a 1D model of arterial system from mass/momentum conservation.
- Young (1808) was the first to identify blood flow with wave-like behavior, and simplify the model.
- Lighthill (1978) and Pedley (1980) first understood pulsatile wave flow (a flow with periodic variations) for blood.

1D or 3D model:

- Low computational cost, thus able study the wave effects within the vascular system as well as isolated segments of an artery.
- Ability to study the effects of arterial modifications, such as placements of stents and prostheses, on pulse waves.
- Easily coupled with lumped parameter models and 3D fluid-structure models.
- System comparison of 1D vs 3D model was conducted. Good agreement between the two models, especially during the diastolic phase of the cycle.

Blood flow model

The one-dimensional blood flow:

$$\begin{cases} A_t + Q_x = 0, \\ Q_t + \left(\frac{Q^2}{A}\right)_x + \frac{A}{\rho}p_x = 0, \end{cases}$$

- $A(x, t) = \pi R(x, t)^2$: cross-sectional area,
- $Q(x, t) = A(x, t)u(x, t)$: discharge,
- $u(x, t)$: flow velocity,
- p : pressure, ρ : blood density.

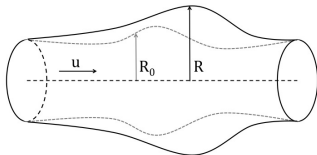
Additional equation to define the pressure: a simple law describing the elastic behavior of the arterial wall

$$p = p_{ext} + K(R - R_0), \quad \text{or equivalently,} \quad p = p_{ext} + \frac{K}{\sqrt{\pi}} \left(\sqrt{A} - \sqrt{A_0} \right)$$

Blood flow model

The one-dimensional blood flow: $\partial_t U + \partial_x f(U) = S(U, A_0)$

$$\underbrace{U = \begin{pmatrix} A \\ Q \end{pmatrix}}_{\text{Conservative Variables}}, \quad \underbrace{f(U) = \begin{pmatrix} Q \\ \frac{Q^2}{A} + \frac{\beta}{3} A^{\frac{3}{2}} \end{pmatrix}}_{\text{Flux Terms}}, \quad \underbrace{S(U, A_0) = \begin{pmatrix} 0 \\ \frac{\beta A}{2\sqrt{A_0}} (A_0)_x \end{pmatrix}}_{\text{Source Terms}}$$



- $A(x, t) = \pi R(x, t)^2$: cross-sectional area
- $Q(x, t) = A(x, t)u(x, t)$: discharge
- $u(x, t)$: flow velocity
- $A_0(x) = \pi R_0(x)^2$: cross-sectional area at rest
- $\beta = \frac{K}{\rho\sqrt{\pi}}$, K : arterial wall stiffness (constant)
- ρ : blood density (constant)

The Well-Balanced Property

Steady States:

Man-at-Eternal-Rest ($u = 0$)

$$\left(u, \sqrt{A} - \sqrt{A_0}\right) = (0, \text{constant}) \quad \text{or} \quad (u, A) = (0, A_0)$$

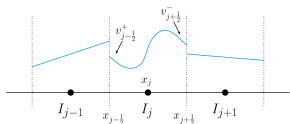
Living-Man ($u \neq 0$)

$$\left(Q, \frac{Q^2}{2A^2} + \beta \left(\sqrt{A} - \sqrt{A_0}\right)\right) = (\text{constant}, \text{constant})$$

Discretization & Fluxes

Mesh Discretization:

- Discretize the domain I into cells
 $I_j = [x_{j-\frac{1}{2}}, x_{j+\frac{1}{2}}]$
- Width of j^{th} cell: Δx_j
- $\tau = \max_j \Delta x_j$



Function Discretization & Projection:

- We seek an approximation U_τ that is a polynomial of degree k in each cell I_j .
- Project the cross-sectional area at rest A_0 into polynomial space as well.
- Project the functions so that $U(x_{j+\frac{1}{2}}) = U_\tau(x_{j+\frac{1}{2}})$ and $A_0(x_{j+\frac{1}{2}}) = (A_0)_\tau(x_{j+\frac{1}{2}})$.

Fluxes:

- A flux takes information from both sides of the cell interface.
- We use the Lax-Friedrichs flux:

$$\hat{f}_{j+\frac{1}{2}} = \frac{1}{2} \left(f(U_{j+\frac{1}{2}}^+) + f(U_{j+\frac{1}{2}}^-) - \alpha \left(U_{j+\frac{1}{2}}^+ - U_{j+\frac{1}{2}}^- \right) \right)$$

DG Numerical Scheme

Begin with the balance law:

$$\partial_t U + \partial_x f(U) = S(U, A_0)$$

Derive the standard DG methods

$$\int_{I_j} \partial_t(U_\tau)(v_\tau) dx - \int_{I_j} f(U_\tau) \partial_x(v_\tau) dx + \hat{f}_{j+\frac{1}{2}} v_\tau(x_{j+\frac{1}{2}}^-) - \hat{f}_{j-\frac{1}{2}} v_\tau(x_{j-\frac{1}{2}}^+) = \int_{I_j} S(U_\tau, (A_0)_\tau)$$

Well-balanced methods for the **Man-at-Eternal-Rest steady state** solution

$$(u, \sqrt{A} - \sqrt{A_0}) = (0, \text{constant}) \quad \text{or} \quad (u, A) = (0, A_0)$$

can be easily designed, following the approach for the shallow water equations.

Next, we focus on the **living-man equilibrium** state

$$\left(Q, \frac{Q^2}{2A^2} + \beta (\sqrt{A} - \sqrt{A_0}) \right) = (\text{constant}, \text{constant})$$

Modified Numerical Scheme

Numerical Scheme in Cell I_j :

$$\begin{aligned} & \int_{I_j} \partial_t U^n v \, dx - \int_{I_j} f(U^n) \partial_x v \, dx + \hat{f}_{j+\frac{1}{2}} v(x_{j+\frac{1}{2}}^-) - \hat{f}_{j-\frac{1}{2}} v(x_{j-\frac{1}{2}}^+) \\ &= \int_{I_j} S(U^n, A_0) v \, dx + (\hat{f}_{j+\frac{1}{2}} - \hat{f}_{j+\frac{1}{2}}^l) v(x_{j+\frac{1}{2}}^-) - (\hat{f}_{j-\frac{1}{2}} - \hat{f}_{j-\frac{1}{2}}^r) v(x_{j-\frac{1}{2}}^+) \end{aligned}$$

which is equivalent to

$$\begin{aligned} & \int_{I_j} \partial_t U^n v \, dx - \int_{I_j} f(U^n) \partial_x v \, dx + \hat{f}_{j+\frac{1}{2}}^l v(x_{j+\frac{1}{2}}^-) - \hat{f}_{j-\frac{1}{2}}^r v(x_{j-\frac{1}{2}}^+) \\ &= \int_{I_j} S(U^n, A_0) v \, dx \end{aligned}$$

with numerical flux: $\hat{f}_{j+\frac{1}{2}} = F(U_{j+\frac{1}{2}}^+, U_{j+\frac{1}{2}}^-)$

Decomposition of U

Transform the conservative variables U into equilibrium variables V :

$$U = \begin{pmatrix} A \\ Q \end{pmatrix} \Rightarrow V = \begin{pmatrix} m \\ E \end{pmatrix} = \begin{pmatrix} Q \\ \frac{Q^2}{2A^2} + \beta(\sqrt{A} - \sqrt{A_0}) \end{pmatrix}$$

Decompose U :

- The equilibrium part (U_τ^e):

$$\hat{V}_j = \begin{pmatrix} \hat{m}_j \\ \hat{E}_j \end{pmatrix} = \begin{pmatrix} m(x_{j+\frac{1}{2}}) \\ E(x_{j+\frac{1}{2}}) \end{pmatrix} \Rightarrow U_\tau^e(x) = \mathbb{P}_\tau U(\hat{V}, A_0(x))$$

- The remaining part (U_τ^r): $U_\tau^r = U_\tau - U_\tau^e$

Important: At a steady state: $U_\tau^e = U_\tau$ and $U_\tau^r = 0$

Numerical Fluxes via Hydrostatic Reconstruction

Define the updated boundary values:

$$U_{j+\frac{1}{2}}^{*, -} = U_{j+\frac{1}{2}}^{-} + U_{j+\frac{1}{2}}^{r, -} \quad U_{j+\frac{1}{2}}^{*, +} = U_{j+\frac{1}{2}}^{-} + U_{j+\frac{1}{2}}^{r, +}$$

Compute the well-balanced numerical fluxes:

$$\begin{aligned}\hat{f}_{j+\frac{1}{2}}^l &= F(U_{j+\frac{1}{2}}^{*, -}, U_{j+\frac{1}{2}}^{*, +}) + f(U_{j+\frac{1}{2}}^{-}) - f(U_{j+\frac{1}{2}}^{*, -}) \\ \hat{f}_{j-\frac{1}{2}}^r &= F(U_{j-\frac{1}{2}}^{*, -}, U_{j-\frac{1}{2}}^{*, +}) + f(U_{j-\frac{1}{2}}^{+}) - f(U_{j-\frac{1}{2}}^{*, +})\end{aligned}$$

where $F(a, b) = \frac{1}{2}(f(a) + f(b) - \alpha(b - a))$ is the Lax-Friedrichs numerical flux.

At the well-balanced state:

$$U_{j\pm\frac{1}{2}}^{*, +} = U_{j\pm\frac{1}{2}}^{*, -} \quad \hat{f}_{j+\frac{1}{2}}^l = f(U_{j+\frac{1}{2}}^{-}) \quad \hat{f}_{j-\frac{1}{2}}^r = f(U_{j-\frac{1}{2}}^{+})$$

The Source Term Approximation

Decompose the source term: $S(U, A_0) = \frac{\beta A}{2\sqrt{A_0}}(A_0)_x = \beta A(\sqrt{A_0})_x$

$$\int S(U, A_0)v \, dx = \int S(U^e, A_0)v \, dx + \int S(U^r, A_0)v \, dx$$

- *The remainder part:* compute directly with quadrature rule
- *The equilibrium part:* approximate

Source term approximation:

$$\begin{aligned} \int_{I_j} S(U, A_0)v \, dx &\approx - \int_{I_j} f(U^e)v_x \, dx + f(U_{j+\frac{1}{2}}^{e,-})v_{j+\frac{1}{2}}^- - f(U_{j-\frac{1}{2}}^{e,+})v_{j-\frac{1}{2}}^+ \\ &+ \int_{I_j} S(U^r, A_0)v \, dx \end{aligned}$$

Verification of Well-Balanced Scheme

The well balanced property is obtained if the residue, R , is zero:

$$\begin{aligned} R &= - \int_{I_j} f(U) \partial_x v \, dx + \hat{f}_{j+\frac{1}{2}}^l v(x_{j+\frac{1}{2}}^-) - \hat{f}_{j-\frac{1}{2}}^r v(x_{j-\frac{1}{2}}^+) \\ &\quad - \left(\int_{I_j} S((U^e)^n, A_0) v \, dx + \int_{I_j} S((U^r)^n, A_0) v \, dx \right) \\ &= - \int_{I_j} f(U) \partial_x v \, dx + f(U_{j+\frac{1}{2}}^-) v(x_{j+\frac{1}{2}}^-) - f(U_{j-\frac{1}{2}}^+) v(x_{j-\frac{1}{2}}^+) \\ &\quad - \int_{I_j} S((U^e)^n, A_0) v \, dx \\ &= 0 \end{aligned}$$

where

- The second equality holds by the consistency of LF flux, design of \hat{f}^l and \hat{f}^r , and $U^r = 0$ at the steady state.
- The third equality is due to the source term approximation.

High-Order Temporal Update Scheme

Scheme: Third order total variation diminishing (TVD) Runge-Kutta time discretization

$$\begin{aligned}U^{(1)} &= U^n + \Delta t \mathcal{F}(U^n), \\U^{(2)} &= \frac{3}{4}U^n + \frac{1}{4}\left(U^{(1)} + \Delta t \mathcal{F}(U^{(1)})\right) \\U^{n+1} &= \frac{1}{3}U^n + \frac{2}{3}\left(U^{(2)} + \Delta t \mathcal{F}(U^{(2)})\right)\end{aligned}$$

where \mathcal{F} is the spatial operator.

Advantages:

- Increased temporal accuracy
- Stability

Tests for Well-Balanced Property

Initial Conditions: $A(x, 0)$ and $Q(x, 0)$ are determined from the equilibrium variables of the steady state and the cross-sectional area at rest A_0 for an artery of length L :

$$Q_s = Q_{in}, \quad E_s = \frac{Q_{in}^2}{2(A_{out})^2} + \beta \left(\sqrt{A_{out}} - \sqrt{A_0(L)} \right),$$

Boundary Conditions: Q_{in} at the inlet & A_{out} at the outlet

Inlet & Outlet Constants:

- Cross-Sectional Area:

$$A_{in} = A_0(0)[1 + 0.5]^2, \quad A_{out} = A_0(L)[1 + 0.5]^2$$

- Discharge: $Q_{in} = A_{in} \times (0.5C_{in})$
- Moens-Kowerteg Wave Coefficient:

$$C_{in} = \sqrt{\frac{K\sqrt{A_{in}}}{2\rho\sqrt{p_i}}}$$

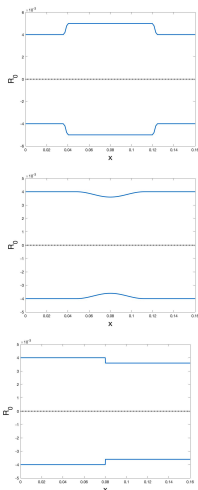


Figure: An aneurysm (top), stenosis (middle), a decreasing step (bottom).

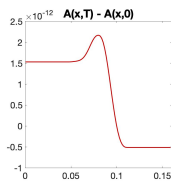
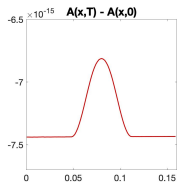
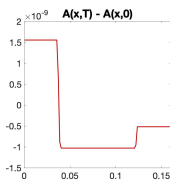
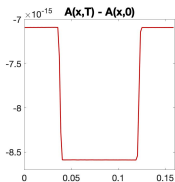
Tests for Well-Balanced Property: Numerical Errors

Living-Man Well-Balanced Scheme						
	Aneurysm		Stenosis		Decreasing Step	
	L^1 Error	L^∞ Error	L^1 Error	L^∞ Error	L^1 Error	L^∞ Error
A	7.360e-15	6.272e-11	8.610e-15	7.420e-11	8.097e-15	6.599e-11
Q	9.851e-15	7.699e-11	1.050e-14	8.203e-11	1.088e-14	8.506e-11

Non-Well-Balanced Scheme						
	Aneurysm		Stenosis		Decreasing Step	
	L^1 Error	L^∞ Error	L^1 Error	L^∞ Error	L^1 Error	L^∞ Error
A	1.168e-09	1.603e-04	7.212e-12	7.312e-07	2.351e-07	4.416e-02
Q	2.045e-09	2.082e-04	6.580e-12	4.830e-07	2.927e-07	2.915e-02

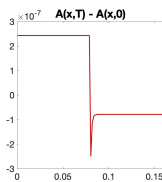
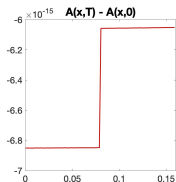
Table: Relative errors for the well-balanced problems at time $t = 5$.

Tests for Well-Balanced Property: Error Plots



(a) *Aneurysm*: Well-balanced (left), non-well-balanced (right)

(b) *Stenosis*: Well-balanced (left), non-well-balanced (right)



(c) *Decreasing Step*: Well-balanced (left), non-well-balanced (right)

Figure: Plot of the errors for the cross-sectional area A .

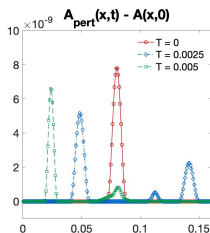
Perturbation to A for Artery with an Aneurysm

Perturbed Initial Conditions of A : $A_{pert}(x, 0) = A(x, 0) + \pi p(x)^2$, with

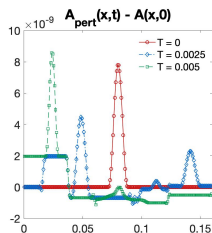
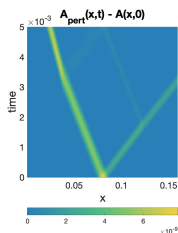
$$p(x) = \begin{cases} 5 \times 10^{-5} \sin\left(\frac{100}{10L} \pi \left(x - \frac{45L}{100}\right)\right), & \text{if } x \in \left[\frac{45L}{100}, \frac{55L}{100}\right], \\ 0, & \text{otherwise} \end{cases}$$

Expected Behavior:

- The perturbation will split into two waves moving in opposite directions.
- Non-inverted reflection waves will appear when the perturbation pulses move into the region of the artery with smaller area.



(a) Well-balanced



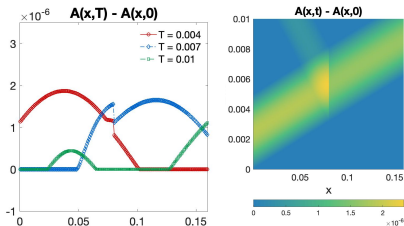
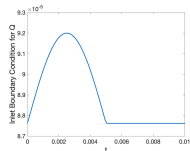
(b) Non well-balanced

Inflow Pulse to Q for an Artery with a Step

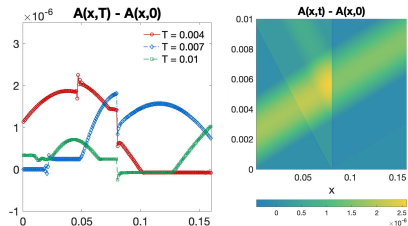
Initial Conditions: Same as in the steady state problems for the step problem.

Perturbed Boundary Conditions: The boundary condition for Q at the inlet:

$$\tilde{Q}_{in}(t) = \begin{cases} Q_{in} (1 + 0.02 \sin(2\pi \frac{t}{T})) & \text{if } t \leq \frac{T}{2}, \\ Q_{in} & \text{otherwise,} \end{cases}$$



(c) Well-balanced



(d) Non well-balanced

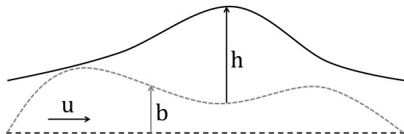
Ripa Model

The Ripa Model (Shallow water equations with horizontal temperature gradients): introduced by Pedro Ripa in 1993

$$\begin{cases} h_t + (hu)_x = 0, \\ (hu)_t + (hu^2 + \frac{1}{2}gh^2\Theta)_x = -gh\Theta b_x \\ (h\Theta)_t + (h\Theta u)_x = 0 \end{cases}$$

Variables:

$h(x, t) \geq 0$	height of the water
$u(x, t) \in \mathbb{R}$	depth-averaged velocity
$\Theta(x, t) > 0$	potential temperature field
$b(x)$	bottom topography function
g	gravitational constant
hu	water discharge
$\frac{1}{2}gh^2\Theta$	pressure that is dependent on the water temperature



Ripa Model

- tsunami and ocean current modeling, river flooding and dam break modeling, atmospheric and planetary flows
- Let $\Theta = 1$, the shallow water equations (SWEs) are recovered

Why to add temperature field Θ ?

- The SWEs assume that the density is constant. Multi-layer SWEs available, when several layers with different constant densities. However, many numerical challenges: complicated eigenstructure, non-conservative terms, and conditional hyperbolicity, etc.
- The Ripa model obtained by vertically averaging over all layers. Lose the information of the interface between layers, but easier in both PDE and numerics. The horizontal temperature gradients are introduced to represent the variations in the fluid density.

Steady State Solutions

Moving water steady state: $u \neq 0$:

$$\begin{cases} hu = \text{constant} \\ \frac{u^2}{2} + g\Theta(h + b) = \text{constant} \\ \Theta = \text{constant} \end{cases}$$

Still water steady state: $u = 0$:

$$\begin{cases} u = 0 \\ \partial_x \left(\frac{1}{2} h^2 \Theta \right) = -h\Theta b_x \end{cases}$$

includes three cases:

- *still-water steady state*

$$(u, \theta, h + b) = (0, C_1, C_2)$$

- *isobaric steady state*

$$(u, b, h^2\theta) = (0, C_1, C_2)$$

- *constant water height steady state*

$$\left(u, h, b + \frac{1}{2} h \ln \theta \right) = (0, C_1, C_2)$$

Well-balanced DG methods

Well-balanced methods for the **still-water steady state** solution

$$(u, \theta, h + b) = (0, C_1, C_2)$$

can be easily designed, following the approach for the SWEs

Similarly, **well-balanced methods** for the **moving-water steady state** solution

$$\begin{cases} hu = \text{constant} \\ \frac{u^2}{2} + g\Theta(h + b) = \text{constant} \\ \Theta = \text{constant} \end{cases}$$

can be designed, following the approach for the SWEs and blood flow (slightly complication due to the third variable)

Well-balanced methods for the **constant water height and isobaric equilibria**, follow the proposed framework to balance the moving-water equilibrium, with some complications detailed in Britton-Xing JSC 2020.

Test for Accuracy

Initial Conditions:

$$\begin{cases} h(x, 0) = 5 + e^{\sin(2\pi x)}, \\ (hu)(x, 0) = \sin(\cos(2\pi x)), \\ \theta(x, 0) = \sin(2\pi x) + 2, \end{cases}$$

Bottom Function: $b(x) = \sin^2(\pi x)$

Boundary Conditions: Periodic

No. Cells	h		hu		$h\Theta$	
	$L^1 Error$	$Order$	$L^1 Error$	$Order$	$L^1 Error$	$Order$
25	7.3659e-04		6.7798e-03		7.8134e-04	
50	1.1235e-04	2.7129	9.0751e-04	2.9013	1.1063e-04	2.8201
100	1.5781e-05	2.8317	1.1708e-04	2.9544	1.8243e-05	2.6004
200	2.0662e-06	2.9331	1.5041e-05	2.9606	2.7879e-06	2.7101
400	2.5592e-07	3.0132	1.8865e-06	2.9951	3.8607e-07	2.8522

Tests for Well-Balanced Property

Bottom Function: $b(x) = \max \{0, 0.2 - 0.05(x - 10)^2\}$

Case 1: Subcritical Flow

Initial Conditions:

$$\begin{cases} m = 4.42 \times \sqrt{5} \\ E = 22.06605 \times 5 \\ \Theta = 5 \end{cases}$$

Boundary conditions:

$$\begin{cases} m = 4.42 \times \sqrt{5} & \text{at upstream} \\ h = 2 & \text{at downstream} \end{cases}$$

	h	hu	$h\Theta$
L^1 Error	3.9850e-13	6.0707e-13	4.0459e-13
L^∞ Error	1.5654e-13	4.2100e-13	1.5965e-13

Case 2: Transcritical Flow

Initial Conditions:

$$\begin{cases} m = 1.53 \times \sqrt{5} \\ E = 11.09098731433671 \times 5 \\ \Theta = 5 \end{cases}$$

Boundary conditions:

$$\begin{cases} m = 1.53 \times \sqrt{5} & \text{at upstream} \\ h = 0.405737258401203 & \text{at downstream} \end{cases}$$

	h	hu	$h\Theta$
L^1 Error	7.2879e-14	3.0429e-13	7.2849e-14
L^∞ Error	8.0269e-14	1.8407e-13	7.6161e-14

Tests for Perturbations

Perturbed Equations:

$$(h_p, (hu)_p, (h\theta)_p)(x, 0) = (h, hu, h\theta)(x, 0) + [0.0001, 0, 0.0005] \chi_{[5.75, 6.25]}.$$

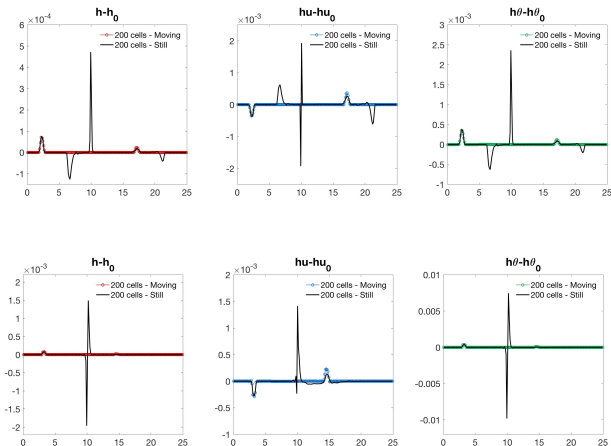


Figure: Plot of errors for the perturbation to the subcritical (top row) and transcritical (bottom row) flow problems at time $t = 0.75$.

Tests for Discontinuous Initial Conditions

Initial Conditions:

$$h(x, 0) + b(x) = \begin{cases} 20 & x < 300 \\ 15 & x \geq 300 \end{cases}, (hu)(x, 0) = \begin{cases} 1 & x < 300 \\ 5 & x \geq 300 \end{cases}, \theta(x, 0) = \begin{cases} 10 & x < 300 \\ 5 & x \geq 300 \end{cases}$$

Bottom Function: $b(x) = \begin{cases} 8 & \text{for } |x - 300| < 75 \\ 0 & \text{otherwise} \end{cases}$

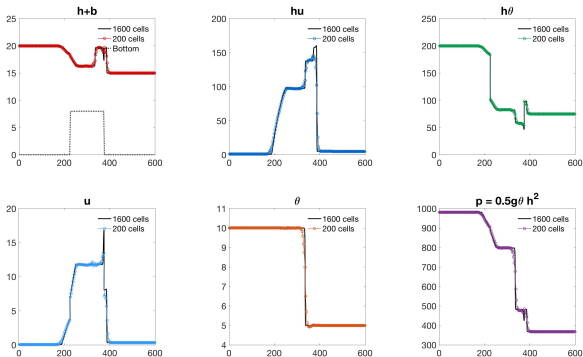


Figure: Numerical solution at time $t = 3$ with a non-constant bottom b .

Chemosensitive Movement Model

Hyperbolic models for chemotaxis

$$\begin{cases} n_t + (nu)_x = 0 \\ (nu)_t + (nu^2 + n)_x = n\chi'(c)\frac{\partial c}{\partial x} - \sigma nu \end{cases}$$

with the chemical concentration $c = c(x, t)$

$$\frac{\partial c}{\partial t} - D_c \Delta c = n - c.$$

$n(x, t)$: cell density, $nu(x, t)$: population flux, σ : friction coefficient.

Modelling that cells change their direction reacting to a chemical substance, approaching chemically favorable environments and avoiding unfavorable ones.

Steady state solution with a zero population flux

$$n\chi'(c)c_x - n_x = 0, \quad nu = 0.$$

where $c = c(x)$ does not depend on t .

Nozzle Flow

Balance laws for a quasi **one-dimensional nozzle flow** through a duct of varying cross-section

$$\begin{cases} (\rho A)_t + (\rho u A)_x = 0 \\ (\rho u A)_t + ((\rho u^2 + p)A)_x = pA'(x) \\ (EA)_t + ((E + p)uA)_x = 0 \end{cases}$$

with the chemical concentration $c = c(x, t)$

$$\frac{\partial c}{\partial t} - D_c \Delta c = n - c.$$

ρ : density, u : velocity, p : pressure, $E = \frac{1}{2}\rho u^2 + \frac{p}{\gamma-1}$: total energy

$A = A(x)$: the area of the cross section

Steady state solution

$$\rho(x, t) = \bar{\rho}(x), \quad p(x, t) = \bar{p}, \quad \text{and} \quad u(x, t) = 0$$

where $\bar{\rho}(x)$ is an arbitrary function in x and \bar{p} is a constant.

Non-equilibrium flow problems

Balance laws for **non-equilibrium flow problems containing finite-rate chemistry or combustion**

$$U_t + F(U)_x = S(U)$$

with

$$U = (\rho_1, \dots, \rho_n, \rho u, \rho e_0)^T,$$

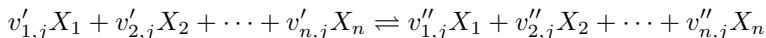
$$F(U) = (\rho_1 u, \dots, \rho_n u, \rho u^2 + p, \rho u e_0 + up)^T,$$

$$S(U) = (s^1, \dots, s^n, 0, 0)^T.$$

with the source term s^i describing the chemical reactions occurring in gas flows (leading to changes in the amount of mass of each chemical species),

$$s^i = M_i \sum_{j=1}^J (v''_{i,j} - v'_{i,j}) \left[k_{f,j} \prod_{s=1}^n \left(\frac{\rho_s}{M_s} \right)^{v'_{s,j}} - k_{b,j} \prod_{s=1}^n \left(\frac{\rho_s}{M_s} \right)^{v''_{s,j}} \right],$$

for the reaction of the form



Zero-Velocity **Steady state solution**

Hydrodynamic equations with general free energy

Balance laws for **hydrodynamic models with attractive-repulsive interaction forces** and linear or nonlinear damping effects (including: phase transitions in collective behavior, Keller-Segel model, and models in chemotaxis, astrophysics, dynamic density functional theories)

$$\rho_t + (\rho u)_x = 0$$

$$(\rho u)_t + (\rho u^2 + p(\rho))_x = -\rho H(x, p)_x - \gamma \rho u - \rho \int_{\mathcal{R}} \phi(x-y)(u(x) - u(y))\rho(y)dy$$

ρ : density, $u(x, t)$: velocity, $P(\rho)$: pressure,

$\phi(x)$: communication function in the Cucker-Smale model

$H(x, \rho)$: attractive-repulsive effects from external V or interaction potential W :

$$H(x, \rho) = V(x) + W(x) \star \rho$$

Zero-Velocity **Steady state solution**:

$$\Pi'(\rho) + H(x, \rho) = \text{constant on each connected component of } \text{supp}(\rho)$$

where $\rho \Pi''(\rho) = P'(\rho)$.

Summary

Constructed and tested **structure-preserving** DG methods for the hyperbolic balance laws

- **Well-balanced** and **positivity-preserving** methods for the Euler equations with gravity:
 - 1 Isothermal equilibrium state,
 - 2 Polytropic equilibrium state,
 - 3 Positivity-preserving limiter, with HLLC flux.
- One dimensional **blood flow** model
- Shallow water equations with **horizontal temperature gradients**
- Examples of other hyperbolic balance laws

High order **finite difference and finite volume WENO methods** can also be designed for these models.

References

- Y. Xing and C.-W. Shu, **High order well-balanced WENO scheme for the gas dynamic equations under gravitational fields**, *Journal of Scientific Computing*, v54 (2013), pp.645-662.
- G. Li and Y. Xing, **Well-balanced discontinuous Galerkin methods for the Euler equations under gravitational fields**, *Journal of Scientific Computing*, v67 (2016), pp. 493-513.
- G. Li and Y. Xing, **High order finite volume WENO schemes for the Euler equations under gravitational fields**, *Journal of Computational Physics*, v316 (2016), pp. 145-163.
- G. Li and Y. Xing, **Well-balanced finite difference weighted essentially non-oscillatory schemes for general equilibrium states of the Euler equations with gravitation**, *Computers and Mathematics with Applications*, v75 (2018), pp. 2071-2085.
- G. Li and Y. Xing, **Well-balanced discontinuous Galerkin methods with hydrostatic reconstruction for the Euler equations with gravitation**, *Journal of Computational Physics*, v352 (2018), pp. 445-462.
- K. Wu and Y. Xing, **Uniformly high-order structure-preserving discontinuous Galerkin methods for Euler equations with gravitation: Positivity and well-balancedness**, submitted.
- J. Britton and Y. Xing, **High order still-water and moving-water equilibria preserving discontinuous Galerkin methods for the Ripa model**, *Journal of Scientific Computing*, v82 (2020), 30.
- J. Britton and Y. Xing, **Well-balanced discontinuous Galerkin methods for the one-dimensional blood flow through arteries model with man-at-eternal-rest and living-man equilibria**, *Computers and Fluids*, v203 (2020), 104493.

Thank you!